UDC 621.3.014.14: 537.528: 533.9.08: 628.16.08: 621.317 https://doi.org/10.20998/2074-272X.2025.1.10

N.A. Shydlovska, S.M. Zakharchenko, M.F. Zakharchenko, M.A. Kulida, S.A. Zakusilo, R.A. Yakovenko

Distribution of volumes of plasma channels components between metal granules in working liquids

Introduction. *Expanding the capabilities of a number of modern technologies and improving quality of their products require detailed spark and plasma erosion processes control in metal granules layers (MGL).* ***Problem.*** *Traditional measurement of exclusively electrical parameters of these processes, even in the case of multi-electrode systems, provides only a general vision, not allowing monitoring processes in individual plasma channels. Optical control methods make it possible to simultaneously have information about almost every plasma channel in the MGL. The* ***aim*** *of the article is to study the characteristic components of plasma channels arising as a result of the flow of discharge currents in the MGL and to establish the laws of distribution of their volumes and their ratios.* ***Methodology****. During the experiments, photographs of plasma channels resulting from the flow of discharge current pulses between Al granules immersed in distilled water were obtained. Using the specialized ToupView program, the volumes of equivalent ellipsoids of rotation, approximating the colored halos and white cores of the plasma channels were determined. Discrete distributions of the volumes of the halo and cores of plasma channels, as well as their ratios were constructed both with and without procedures for screening out «anomalous» results. The efficiency of approximation of discrete distributions obtained in practice by continuous theoretical distributions Weibull, Rosin-Rammler and log-normal was estimated.* ***Results.*** *It is shown that of all the considered theoretical distributions of halo and cores of plasma channels volumes, as well as their ratios, the most adequate is the log-normal one.* ***Originality.*** *For the first time distributions of volumes of halo and cores of plasma channels were studied and their comparative analysis with the size distributions of erosion particles and dimples on the surface of Al granules was given.* ***Practical significance.*** *Taking into account the new obtained results, a technique for constructing distributions of volumes of halo and cores of plasma channels and determining their parameters has been developed.* References 53, figures 7, tables 5.

Key words: **plasma channels, spark, discharge current, statistical distributions, metal granules, erosion particles.**

Вступ. *Розширення можливостей та підвищення якості продукції іскроерозійних технологій потребує залучення не тільки електричних, а і оптичних методів контролю процесів.* ***Проблема.*** *Створення методів керування властивостями іскроерозійних частинок на основі даних оптичних вимірювань потребує вирішення декількох науково-практичних задач.* ***Мета.*** *Визначення законів розподілу об'ємів кольорових гало та білих іскрових ядер плазмових каналів, які виникають у шарі гранул металів в результаті протікання імпульсних розрядних струмів.* ***Методологія.*** *Аналіз якості апроксимації отриманих в ході експериментів розподілів об'ємів складових плазмових каналів низкою теоретичних розподілів.* ***Отримані результати.*** *Найбільш адекватним серед усіх розглянутих теоретичних законів, що описують розподіли об'ємів гало і ядер плазмових каналів, а також їхніх відношень, є логарифмічно-нормальний.* ***Оригінальність.*** *Вперше досліджено розподіли об'ємів гало і ядер плазмових каналів та наведено їх порівняльний аналіз з розподілами розмірів ерозійних частинок і лунок на поверхні гранул Al.* ***Практична значимість.*** *Розроблено методику побудови розподілів об'ємів гало і ядер плазмових каналів.* Бібл. 53, рис. 7, табл. 5.

Ключові слова: **плазмові канали, іскра, розрядний струм, статистичні розподіли, металеві гранули, ерозійні частинки.**

Introduction and research problem definition. The formation of plasma channels as a result of the flow of pulsed discharge currents between the surfaces of adjacent metal and alloy granules in their layers, which are in working fluids, is the electrophysical basis of a number of technological processes. The most common of them can be classified into four main groups.

The first includes the production of microdispersed powders of metals and alloys with special properties: heat-resistant and refractory [1], hard [2], soft magnetic [3], amorphous [4, 5], with shape memory [6], corrosion-resistant [7], etc. [8, 9]. The second includes electric discharge sintering of metal powders under pressure [10]. The third is the production of nanodispersed hydrosols of biocidal metals (*Ag*, *Cu*, *Zn*) for use in veterinary medicine [11] and biogenic metals (*Fe*, *Mg*, *Mn*, *Co*, *Mo*) for use in crop production [12]. The fourth is the production of *Al* and *Fe* hydroxides for purification [13] and disinfection [14] of natural waters, including for the needs of thermal and nuclear power engineering [15].

The key parameters of discharge pulses: their duration [16], number of modes [17], average power over the pulse time [18], amplitude and shape [19, 20] of the discharge current and voltage on the metal granules layers (MGL) together with the technological conditions of the above processes [21] determine the properties of the products obtained [22]. Until now, the basis for controlling the processes described above has been the control and maintenance within certain limits of the values of some parameters of discharge pulses averaged over a certain time: the amplitudes of current and voltage, their duration and repetition frequency, as well as the height of the MGL, the flow rate and the temperature of the working fluid in the discharge chamber [18, 21–23].

Depending on the ratio of the dimensions of the discharge chamber (DC) and the metal granules contained in it, their number in the active zone of the chamber can reach 100 thousand. Under such conditions, it is impossible to control at least one parameter of the discharge pulse in each individual plasma channel by traditional measurements of electrical quantities, even in the case of multi-electrode systems [24]. The large number of places of probable occurrence of plasma channels and the quasi-identity of conditions at each level

of the MGL height [21] are the basis for involving statistical methods for studying these processes [25].

Unlike measuring discharge current parameters, measuring plasma channel parameters by optical methods allows obtaining information about the vast majority of them simultaneously. The number of plasma channels that can be observed simultaneously depends on the number of granules in each observation direction, their packing density in the layer, and the transparency of the working fluid [26].

As is known, the flux of electromagnetic radiation in both the radio frequency and infrared, optical and ultraviolet ranges is proportional to the power of the electric current emitted in the plasma channel [27–33]. Therefore, by studying such components of the radiation flux as the size of the luminous areas, their energy luminosity and the radiation spectrum, it is possible to obtain information about the power emitted in each plasma channel, and knowing the dependence of the radiation flux on time, it is also possible to obtain information about the energy on which the size of the eroded metal particles and the productivity of their production depend [16, 22].

The correlation between the components of the radiation flux of plasma channels and the size of the eroded particles, as well as their dependence on the parameters of the discharge pulses, will form the theoretical basis of the laws of regulating the properties of particles by the parameters of the plasma channels. This is a difficult task, which is solved in several stages. At the first stage, it is necessary to determine the laws of volume distributions of the components of plasma channels in the MGL.

The aim of the work is to study the characteristic sections of plasma channels that arise as a result of the flow of discharge currents in the MGL, to establish the discrete and theoretical continuous laws of their volume distributions and their correlations obtained in practice, and to find the parameters of these laws.

Experimental methodology, equipment, modes and materials. The objects of research were spark cores of plasma channels between *Al* granules in distilled water formed as a result of the action of discharge currents, which had a continuous white emission spectrum and colored halos around them, which had a linear emission spectrum [26]. Halos are caused by streamer and leader channels [34–36] at the early stages of the evolution of plasma channels, and their emission can also be induced by ultraviolet radiation of spark cores. This issue is discussed in more detail in [26]. There is also a functional diagram of the laboratory equipment on which the experiments were conducted and a detailed description of its operation. Here we will give only a brief description of the equipment and its operating modes.

The thyristor discharge pulse generator provided a free aperiodic discharge of a working capacitor with capacitance of C=100 μF with fixed pulse repetition rate f=50 Hz. The inductance of the discharge circuit of the generator was L=2 μH, and the resistance of the resistive shunt R=3 Ω. The shunt was connected in parallel with the DC to reduce the probability of simultaneous current flow in the charging and discharging circuits of the generator due to the delay of the discharge process due to a stochastic increase in the resistance of the MGL. The average values of the amplitudes of the voltage pulses on the MGL were approximately U_m≈220 V, and the current in it I_m≈180 A. The average pulse duration τ was about 100 μs.

The A7E aluminum granules, the surface of which had previously undergone spark discharge treatment, had a quasi-spherical shape with a diameter of approximately 4 mm. The distance between the vertical AD0 grade aluminum electrodes in the DC was 52 mm. The height of the MGL was 30 mm, and its width was 22 mm. The water flow was directed from bottom to top and was approximately 12 ml/s, which ensured the stability of the process and removed erosion particles from the active zone of the DC without significant movement of the aluminum granules in it. To record images of the constituent plasma channels, a household webcam with a matrix of 640×480 pixels was used in video recording mode. The resulting video stream was then decomposed into separate frames, the images of the plasma channels on which were analyzed using the specialized ToupView program [37], which is freely available and is designed to work with digital optical cameras of microscopes and telescopes. The images of the cores and halos were approximated by ellipses of equivalent area, and the sizes of their major *2a* and minor *2b* axes were automatically calculated by the program. Then, the volumes of equivalent ellipsoids of rotation were calculated from them. This procedure is described in more detail in [26].

Optometric analysis of the volumes of the plasma channels components. One of the many frames obtained and processed using the above-described method is shown in Fig. 1. It shows the plasma channels existing during the discharge pulse between aluminum granules immersed in distilled water, which are in the dark, which is necessary to increase the contrast. The ellipses equivalent in area, which were used to approximate the projections of the spark cores of the plasma channels onto the plane of the webcam, are red in color, and their colored halos are blue. In [26] the continuous spectrum of white emission of spark cores and the linear blue-violet spectrum of emission of colored halo plasma channels containing aluminum atoms and their compounds with oxygen and hydrogen were substantiated. This makes it possible to determine the sizes of the corresponding zones in Fig. 1 by their brightness and color, although this process contains a certain element of subjective assessment. In the printed version of the article, the figures are presented in grayscale. Color versions are available on the website of the Journal «Electrical Engineering & Electromechanics».

The ToupView program automatically generates service labels: the designation of the ellipse (capital letter E), its serial number (for spark cores it is odd, starting with 1, and for color halos it is even, starting with 2), the values of the lengths of the major 2*a* and minor 2*b* axes of the ellipses, written through commas and units of measurement (in this case px – pixels). That

is, in a pair of serial numbers, the smaller odd number will correspond to the equivalent in area ellipse projection of the spark core of the plasma channel, and the next even number will correspond to its color halo. Thus, 134 ellipses were obtained with the values of the lengths of their axes, which approximate, respectively, the spark cores and color halos of 67 plasma channels. This number is sufficient to speak about the approximation of the frequency of observation cases to their probability and to construct histograms of discrete distributions of plasma channel volumes obtained during experiments [25, 38, 39].

The width of the image in Fig. 1 corresponds to the width of the MGL in the DC (the electrodes are outside the frame), which is approximately 50 mm. At the same time, the width of the image in the ToupView program is 162 px. This means that one millimeter of a real object corresponds to approximately 3.2 px of the image in the ToupView program. This coefficient was used to convert the sizes of objects from pixels to millimeters in the Microsoft Office Excel 2003 program during further processing of the measurement results.

In [26] it is shown that to determine the volumes of the components of plasma channels under the above conditions, they can be represented by equivalent ellipsoids of rotation, the dimensions of the axes of which are located on their projections onto the plane of the webcam. The camera is located in a plane perpendicular to the planes of the electrode surfaces, i.e. parallel to the planes of flow of the vast majority of discharge currents in the MGL. Therefore, in most cases, from such a perspective, the true size of the axes of the equivalent ellipsoids of rotation is observed without distortion. And in the case of the coincidence of the directions of the corresponding axes of the spark core and color halo ellipsoids, their ratio, as well as the ratio of the volumes of the corresponding ellipsoids, do not depend on the observation perspective [26].

Unfortunately, from the analysis of a 2D image of plasma channels it is impossible to accurately determine which of the two axes of the projection of the equivalent ellipsoid is its axis of rotation or its projection. If the dimensions of the micro-roughness on the surface of the granules are significantly smaller than the distance between adjacent granules, it is more likely that the major axis of the ellipse 2*a* is the axis of rotation of the ellipsoid or its projection and the ellipsoid of rotation is «elongated». The volumes of the equivalent ellipsoids of the plasma channels in this case are denoted by the index *a*. This situation is more typical for the upper layers of the granules, in which the pressure on the granules is lower.

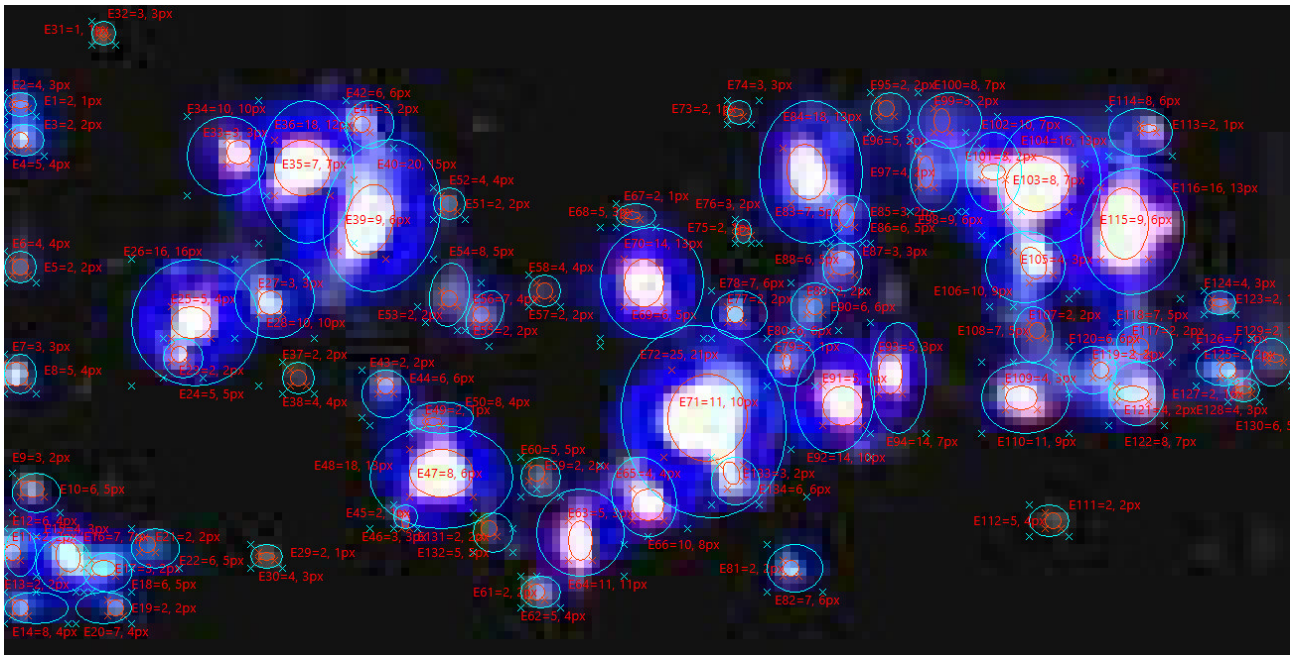

Fig. 1. Plasma channels between aluminum granules in water in the dark

In another case, when the dimensions of micro-roughnesses on the surface of the granules are commensurable to the distance between neighboring granules, with a higher probability the minor axis of the ellipse 2*b* is the axis of rotation of the ellipsoid or its projection and the ellipsoid of rotation is «flattened». In this case, the volumes of equivalent ellipsoids of the constituent plasma channels are denoted by the index *b*. This situation is more typical for the lower layers of the granules, in which the pressure on the granules is greater.

In real conditions, both options are possible, therefore, when analyzing the volumes of equivalent ellipsoids of rotation of the constituent plasma channels, calculations of their volumes were carried out for both cases (indexes *a* and *b*, respectively). The volume of the ellipsoid of rotation, equivalent to the volume of the spark core of the plasma channel (index s) for two cases of the position of the rotation axis (major axis 2*a* or minor axis 2*b*) according to the well-known formula [40] was determined:

$$V_s = \begin{cases} V_{sa} = 4\pi a_L b_L^2/3, \text{ if } 2a - \text{axis of rotation;} \\ V_{sb} = 4\pi b_L a_L^2/3, \text{ if } 2b - \text{axis of rotation.} \end{cases} \quad (1)$$

The volumes of colored halos (denoted by the index L) were assumed to be the difference of the total volumes of plasma channels and their spark cores and were calculated for the two cases of the rotation axis position as:

$$V_L = \begin{cases} V_{La} = 4\pi\left(a_L b_L^2 - a_s b_s^2\right)/3, \text{ if } 2a - \text{rotation;} \\ V_{Lb} = 4\pi\left(b_L a_L^2 - b_s a_s^2\right)/3, \text{ if } 2b - \text{rotation.} \end{cases} \quad (2)$$

The ratios of the volumes of colored halos to the volumes of spark channels for two cases of the position of the rotation axis were calculated based on (1), (2) according to the expression:

$$V_L/V_s = \begin{cases} V_{La}/V_{sa} = \left(a_L b_L^2/a_s b_s^2\right) - 1, \text{ if } 2a - \text{rotation;} \\ V_{Lb}/V_{sb} = \left(b_L a_L^2/b_s a_s^2\right) - 1, \text{ if } 2b - \text{rotation.} \end{cases} \quad (3)$$

For two cases of the position of the rotation axis (coincides with the major axis $2a$ or coincides with the minor axis $2b$), the volumes of the rotation ellipsoids V_{sa} and V_{sb}, respectively, equivalent to the volumes of the spark cores of 67 plasma channels, (2) equivalent to the volumes of their color halos V_{La} and V_{Lb}, respectively, and (3) the ratios of the volumes of these regions of the channels V_{La}/V_{sa} and V_{Lb}/V_{sb}, respectively, were calculated by (1).

Statistical analysis of the distributions of the volumes of the components of plasma channels. For each sample of these volumes and their ratios with a total number of N elements, the following statistical moments were calculated: the mathematical expectation over the sample [41]:

$$M_S[V] = \frac{1}{N}\sum_{j=1}^{N} V_j , \quad (4)$$

the sample variance:

$$D_S[V] = \frac{1}{N}\sum_{j=1}^{N}\left(V_j - M_S[V]\right)^2 , \quad (5)$$

and the coefficient of variation for the sample:

$$\nu_S[V] = \sqrt{D_S[V]}/M_S[V] . \quad (6)$$

In the process of constructing discrete distributions of the above random variables, the following parameters were determined based on the measurement results: the minimum $V_{\min}$ and maximum $V_{\max}$ values of the corresponding volumes and their ratios by samples, the number of their values in each sample N, the number of intervals of discrete distributions n, the number of values in each interval N_j, the proportion in each interval $n_j=N_j/N$, the average value of the volume (or the ratio of volumes) $\overline{V}_{nj}$ in each j-th interval of discrete distributions, the mathematical expectation for the discrete distribution:

$$M_D[V] = \sum_{j=1}^{n} n_j \overline{V}_{nj} , \quad (7)$$

the variance according to the discrete distribution:

$$D_D[V] = \sum_{j=1}^{n} n_j\left(\overline{V}_{nj} - M_D[V]\right)^2 , \quad (8)$$

and the coefficient of variation for the discrete distribution:

$$\nu_D[V] = \sqrt{D_D[V]}/M_D[V] . \quad (9)$$

The rounded values of the above parameters are given in Table 1. The units of measurement of volumes and their mathematical expectations in Table 1 – mm^3, of variances of their distributions – mm^6, and the volume ratios and coefficients of variation are dimensionless quantities.

Table 1

Statistical parameters of sample volumes of plasma channels components and their ratios

Sample	$V_{\min}$	$V_{\max}$	N	$M_S[V]$	$D_S[V]$	$\nu_S[V]$	$M_D[V]$	$D_D[V]$	$\nu_D[V]$
V_{sa0}	0,02	17,57	67	0,96	6,20	2,61	1,78	4,24	1,16
V_{sa1}	0,02	6,26	66	0,70	2,05	2,03	0,94	1,80	1,42
V_{sa2}	0,02	2,80	61	0,32	0,29	1,65	0,39	0,22	1,21
V_{sb0}	0,02	19,34	67	1,17	8,36	2,47	2,09	5,76	1,15
V_{sb1}	0,02	7,77	66	0,89	3,41	2,07	1,16	2,73	1,42
V_{La0}	0,16	158,6	67	11,31	549,2	2,07	17,21	372,5	1,12
V_{La1}	0,16	66,73	66	9,08	223,8	1,65	10,81	174,8	1,22
V_{Lb0}	0,22	190,4	67	14,00	820,0	2,05	22,35	645,1	1,14
V_{Lb1}	0,22	88,11	66	11,32	353,9	1,66	14,11	300,6	1,23
$(V_{La}/V_{sa})_0$	1,96	143,0	67	21,79	499,9	1,03	22,26	489,3	0,99
$(V_{La}/V_{sa})_1$	1,96	74,00	65	18,62	167,5	0,70	18,68	155,1	0,67
$(V_{Lb}/V_{sb})_0$	2,70	92,30	67	19,92	239,4	0,78	19,93	224,6	0,75
$(V_{Lb}/V_{sb})_1$	2,70	63,00	66	18,79	156,4	0,67	18,77	150,0	0,65

As can be seen from Table 1, the statistical moments for samples (4) – (6) differ from the corresponding statistical moments for discrete distributions (7) – (9). This is due to the process of discretization of distributions of relatively small numbers of sample elements. Statistical moments for samples are primary information, therefore they more accurately reflect the parameters of the distributions.

When determining the optimal number of intervals of discrete distributions n [42], it is recommended to use the ratio $n \le \text{int}\left[\sqrt{N}\right]$. In the case of a uniform distribution, this ratio provides approximately the same number of distribution intervals and random variable values in each of them, which leads to close values of discretization errors both for intervals and for values in them. In addition, it is recommended that the number of intervals of the discrete distribution be in the range from 6 to 20. If the distribution is quasi-symmetric, then it is better to choose an odd number of its intervals. In the distributions considered here, N lies in the range from 61 to 67 (Table 1), therefore, taking into account the above, n=7 was chosen for all distributions.

When constructing discrete distributions based on the results of measurements of random variables, an important operation is to screen out «anomalous» values of the input data [43]. The distributions of the measurement results of any variable obtained in practice under quasi-identical conditions may differ significantly from the theoretical distributions of a random variable for such conditions. This may be due to a number of reasons.

Firstly, due to measurement errors, as a result of which some values of a random variable differ significantly from its mathematical expectation. Secondly, due to an insufficient number of measurements, which leads to inaccurate determination of the mathematical expectation, dispersion and other moments and parameters of the distributions of a random variable. Thirdly, due to an uncontrolled change in the parameters of real processes that affect the measurement results and violate the quasi-identicality of the experimental conditions. This can lead to the appearance of a certain number of «anomalous» measurement results, which make it impossible to qualitatively approximate discrete distributions obtained in practice by continuous theoretical distributions.

Several statistical criteria for screening out «anomalous» measurement results are known. Among them: Grubbs criteria [44], $2m$ – $3m$, Wright (another name 3σ) [45], $\acute{Z}$, Dixon, Charlier, Student coefficients, Irwin, etc. [43, 46]. But none of them guarantees screening out all «anomalous» results and preserving all error-free, and even more so eliminating all areas with zero values in the body of experimental distributions. In [43] it is shown that one of the most effective criteria for screening out «anomalous» measurement results is Wright criterion, which is why we used it in our studies.

In Table 1 – 5, the index «0» denotes the input samples without screening out «anomalous» measurement results. In Tables 1 – 5, their parameters are given in shaded rows. The index «1» denotes the samples in which screening out «anomalous» measurement results occurred in one iteration according to the Wright criterion. The index «2» denotes the sample in which screening out «anomalous» measurement results occurred in two iterations until all areas with zero values in the body of the experimental distributions were eliminated.

The screening out of «anomalous» measurement results according to the Wright criterion narrows the range of values that most of the considered random variables can take by more than 2 times, and screening out until all areas with zero values are eliminated by more than 6 times (Table 1). In all the considered samples, the largest values of the measured variables were screened out. The probability of measurement error of the largest values is much smaller than that of the smallest. When performing the screening operations, the mathematical expectations and variances, both for samples and for discrete distributions, as well as the coefficients of variation for samples, are noticeably reduced. These facts suggest that the values are screened out incorrectly.

The distributions of the volumes of spark cores, colored halos and their ratios are shown in Fig. 2 – 7. The discrete distributions obtained directly as a result of experiments are represented by histograms. The theoretical continuous distributions obtained from them, the values of the parameters of which are found by the method of statistical moments of the input samples, are represented by curves. The distributions for the cases when the major axes of the ellipsoids are their axes of rotation are shown in blue, and when they are minor are shown in red. The points at which the values of the theoretical distributions were calculated are marked in Fig. 2 – 7 with triangles with vertices at the top for cases when the major axes of the ellipsoids are their axes of rotation, and with the vertex at the bottom – when they are minor. Figures 2, 4, 6 present the distributions for all arrays of the obtained data without prior screening, and Fig. 3, 5, 7 – for data that have undergone preliminary screening according to the Wright criterion.

From the comparison of the pairs of Fig. 2 and Fig. 3, Fig. 4 and Fig. 5 and Fig. 6 and Fig. 7 it is seen that in all the considered cases, screening out of «anomalous» measurement results according to the Wright criterion does not lead to an improvement in the appearance of the distributions. Moreover, screening of the results significantly distorts the appearance of the distributions of the ratios of the volumes of colored halos to spark cores in Fig. 7 in comparison with Fig. 6.

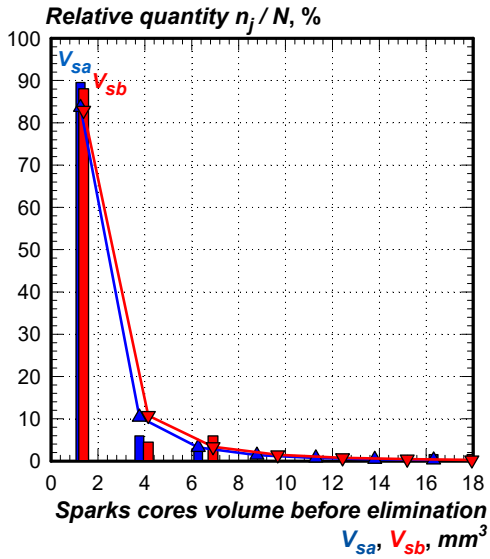

Fig. 2. Distributions of spark cores volumes before screening out

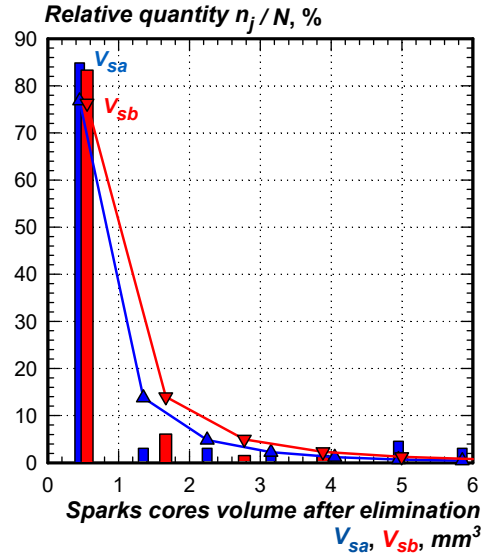

Fig. 3. Distributions of spark cores volumes after screening out

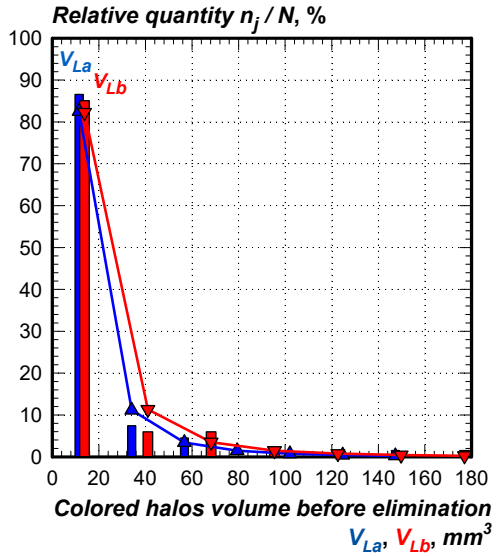

Fig. 4. Distributions of colored halo volumes before screening out

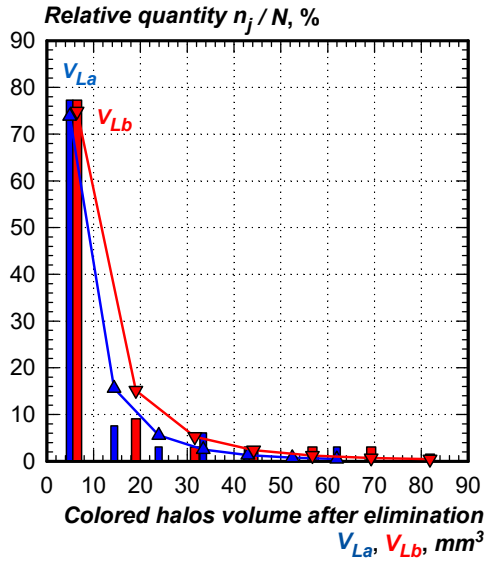

Fig. 5. Distributions of colored halo volumes after screening out

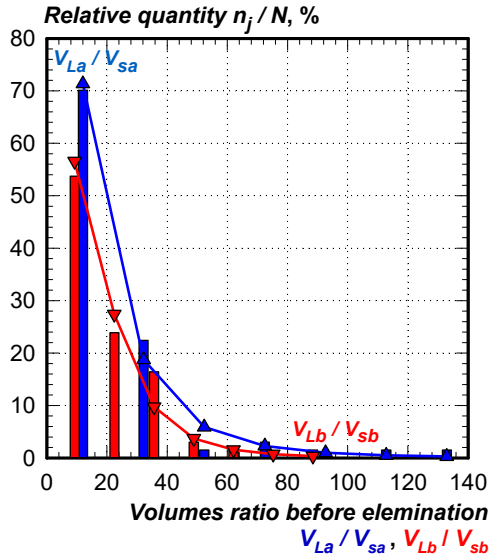

Fig. 6. Distributions of ratios of volumes of colored halos to volumes of spark cores before screening out

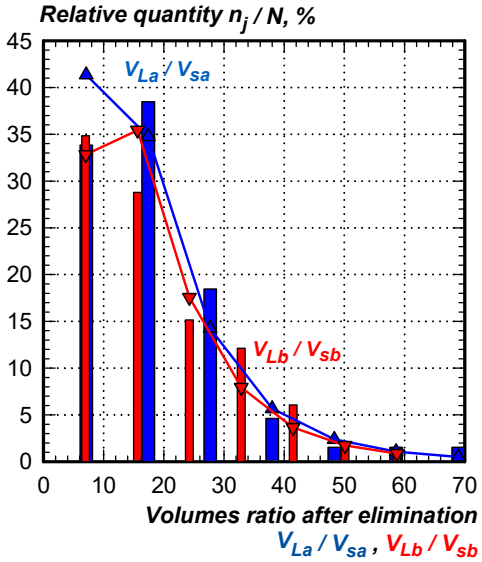

Fig. 7. Distributions of ratios of volumes of colored halos to volumes of spark cores after screening out

All distributions in Fig. 2, 4, 6 have similar shapes, which suggests that they can be described by one theoretical distribution with different parameter values. The volume distributions in which the equivalent ellipsoids were considered «flattened», i.e. the rotation axis was small (denoted by the index *b*) are more monotonic and match the theoretical distributions better than the volume distributions in which the equivalent ellipsoids were considered «elongated», i.e. the rotation axis was large (denoted by the index *a*). This is best seen in Fig. 6 for the distributions of the ratios of the volumes of colored halos to spark cores. This suggests that under the considered conditions, most of the components of the plasma channels are more correctly approximated by «flattened» rotation ellipsoids than by «elongated» ones.

The values of the volumes of the «flattened» ellipsoids in Fig. 2 – 5 were always slightly larger than the values of the volumes of «elongated» ellipsoids under the same conditions, which follows from the analysis of (1), (2). As for the ratios of the volumes of colored halos to spark cores (Fig. 6, 7), the opposite trend is observed there.

Approximation of the distributions of the volumes of the components of plasma channels and their ratios by theoretical distributions. Based on the type of discrete distributions, the values of their coefficients of variation, and the most typical cases of application of theoretical distributions [47], the following were considered to find the best one: log-normal, Weibull, and Rosin-Rammler [48].

The probability density of a random variable V according to the log-normal law is determined [49]:

$$f_{LN}(V)=\frac{1}{V\alpha\sqrt{2\pi}}\exp\left[-\frac{(\ln V-\mu)^2}{2\alpha^2}\right], \qquad (10)$$

where $\alpha=\sqrt{\ln\left[D[V]/M^2[V]+1\right]}$ is the standard deviation of the natural logarithms of a random variable;

$\mu = \ln\left[M[V] \Big/ \sqrt{D[V] \Big/ M^2[V] + 1} \right]$ is the average of the natural logarithms of a random variable.

The probability density of a random variable V according to the Weibull distribution [50]:

$$f_W(V) = \begin{cases} \frac{w}{\lambda}\left(\frac{V}{\lambda}\right)^{w-1} \exp\left[-\left(\frac{V}{\lambda}\right)^{w}\right], & V \geq 0; \\ 0, & V < 0, \end{cases} \quad (11)$$

where w is the shape factor; λ is the scale factor.

The probability density of a random variable V according to the Rosin-Rammler distribution is determined [51]:

$$f_R(V) = \begin{cases} 1 - \exp\left[\ln(0{,}2) \cdot (V / P_{80})^m\right], & V \geq 0; \\ 0, & V < 0, \end{cases} \quad (12)$$

where P_{80} is the 80th percentile of the distribution; m is the distribution range parameter.

The theoretical distributions we have considered are given on the intervals of change of the random variable $V \in (0; +\infty)$ for (10) and on $V \in [0; +\infty[$ for (11) and (12), while the distributions obtained in the course of experiments are given on much smaller intervals (Table 1). Therefore, to ensure the value of 100 % of the distribution functions in the real intervals of change of their arguments, the probability density of each theoretical distribution law $f(V)$ in each case must be multiplied by the corresponding correction coefficients of the ranges:

$$k = 100\% \Big/ \int_{V_{\min}}^{V_{\max}} f(V) \mathrm{d}V . \quad (13)$$

Finding the optimal values of the parameters of the theoretical distribution laws was carried out using two main groups of methods: statistical moments and the least deviation of theoretical values from the experimental results [48].

Statistical moments methods, unlike the methods of the least deviation of theoretical values from the experimental results, give unambiguous results, and not an infinite number of groups of parameters of the distribution laws. Therefore, if possible, these methods should be preferred.

However, in situations where the number of sample elements is relatively small, as in our studies, it is very difficult to accurately calculate the values of the parameters of the Rosin-Rammler and Weibull distributions using the first group of methods. For example, it is almost impossible to accurately find the value of P_{80} using our samples. Then the second group of methods comes in handy. For each j-th interval of the discrete distributions obtained as a result of the experiments, the differences between the number of objects observed in it n_{jO} and the number of objects that should be in it according to the continuous theoretical distribution law n_{jE} were found. Using all the obtained differences in accordance with the selected optimization function, its value was calculated. Then, using the «Solver» add-in of the English-language program Microsoft Office Excel 2003, the search for optimal values of the parameters of the theoretical distribution laws was performed under the condition of the smallest value of the selected optimization function.

We used the following as such functions: sum of squared differences (SSD) of the values of the discrete and continuous theoretical distributions obtained during the experiment:

$$S = \sum_{j=1}^{n} \left(n_{jO} - n_{jE}\right)^2 , \quad (14)$$

Pearson Chi-squared consistency criterion [52]:

$$\chi_n^2 = \sum_{j=1}^{n} \left(n_{jO} - n_{jE}\right)^2 \Big/ n_{jE} , \quad (15)$$

and the average modulus of relative deviations of the values obtained during the experiments of the discrete and continuous theoretical distributions:

$$|\delta| = \frac{100\%}{n} \sum_{j=1}^{n} \left| \left(n_{jO} - n_{jE}\right) \Big/ n_{jO} \right| . \quad (16)$$

The SSD (14) is one of the oldest optimization functions in the processes of finding coefficients of approximating functions. It is very easy to use and does not require large amounts of calculations. However, it is necessary to pay attention to the shortcomings of the SSD as an optimization function and as a criterion of the quality of approximation. The SSD uses squares of absolute, not relative, estimates, therefore, the quality of approximations under the condition of the minimum value of the SSD will be higher in those areas where the approximating function has large values and lower in areas where its values are small. The dependence of the SSD on the number of its members makes it not universal when comparing approximations of discretely given dependencies with different numbers of elements.

Traditionally, the possibility of using continuous theoretical distributions to approximate discrete distributions obtained as a result of experiments was assessed using the Pearson Chi-squared consistency criterion (15). Therefore, its choice as an optimization function is quite logical. But criterion (15) is also not without its shortcomings. Although, unlike (14), criterion (15) has a denominator, in its numerator there is the square of the difference. That is, criterion (15), like (14) is not dimensionless and universal. In addition, like (14) it depends on the number of intervals of the discrete distribution.

Among all the expressions considered here for optimization functions and criteria for the quality of approximation (14) – (16), only the average modulus of relative deviations (16) is universal. It provides a relative estimate, is dimensionless and does not depend on the number of elements of the discrete dependence. When using it as an optimization function, it should be noted that the quality of approximation in areas with small values of the approximating function may be higher than in areas with its large values. This is due to the use of relative, not absolute, estimates.

The disadvantage of the group of methods of the least deviation of theoretical values from the results of experiments is the ambiguity of the obtained results, due to the fact that the number of equations, which

corresponds to the number of intervals of discrete distributions, is greater than the number of parameters of theoretical distributions. That is, the system of equations is redundant and can have an infinite number of solutions (combinations of the values of the parameters of theoretical distribution laws). This leads to different results obtained by different optimization functions for the same distributions (Tables 2 – 4). The parameter values obtained in this way may be inconvenient for further calculations and be far from the values determined by the physical content of the quantities under study.

For all thirteen samples (Table 1), the values of the range coefficients (13) and the Pearson Chi-squared consistency criterion (15), found by the methods of the smallest values of the SCR (14), Chi-squared (15) and the average modulus of relative deviations (16), as well as the parameters of the theoretical distribution laws are given in Table 2 – 4. For the Weibull distribution – in Table 2, Rosin-Rammler – in Table 3, log-normal distribution – in Table 4. The decision on the correspondence or inconsistency of the theoretical law with the experimental data was made using the classical method of rejecting or accepting the null hypothesis about the consistency of the frequencies of occurrence of a discrete random variable in the specified intervals of its distribution, which were obtained during the measurement, and the values of the theoretical density functions of the distributions of continuous random variables. The significance of the first-order error ξ of the rejection of the null hypothesis when it is true, that is, when the theoretical distribution is rejected, and in fact it is consistent with the experimental data, was set at the level of $\xi = 0.05$. The number of degrees of freedom of the Chi-squared distribution is determined by $\zeta = n–1$ and in the considered distributions is: $\zeta = 7–1 = 6$.

The value of the critical point of the Chi-squared distribution was calculated using the built-in function CHIINV(ξ; ζ) of the English-language program Microsoft Office Excel 2003 and for $\xi = 0.05$ and $\zeta = 6$ it is approximately $\chi_k^2 \approx 12.5916$. That is, if the values found by (15) are less than 12.5916, then with a significance level of the first-order error $\xi = 5$ %, the null hypothesis is not rejected and the theoretical distribution with the current parameters passes according to the Pearson Chi-squared consistency criterion (marked «pass» in Tables 2 – 4 and «p» in Table 5).

In cases where the values found by (15) are greater than $\chi_k^2 = 12.5916$, with a significance level of the first-order error $\xi = 5$ %, the null hypothesis is rejected and the theoretical distribution with the current parameters is failed according to the Pearson Chi-squared consistency criterion (marked «fail» in Table 2 – 4 and «f» in Table 5).

Table 2

Weibull distribution parameters found by least-value methods of three different optimization functions

Sample	min [S]					min [χ_n^2]					min [$\lvert\delta\rvert$]				
	w	λ	k, %	χ_n^2	p / f	w	λ	k, %	χ_n^2	p / f	w	λ	k, %	χ_n^2	p / f
V_{sa0}	0,3175	0,0413	4,7687	7,0	pass	0,3175	0,0413	4,7687	7,0	pass	0,2676	0,1033	8,8405	16,708	fail
V_{sa1}	0,2629	0,0222	20,466	17,0	fail	0,2629	0,0222	20,466	17,0	fail	0,2192	0,0625	27,132	22,287	fail
V_{sa2}	0,2629	0,0222	61,081	6,2162	pass	0,2629	0,0222	61,081	6,2162	pass	0,2629	0,0222	61,081	6,2162	pass
V_{sb0}	0,2417	0,0052	1,7299	7,9	pass	0,2417	0,0052	1,7299	7,9	pass	0,2117	0,0182	4,6001	14,974	fail
V_{sb1}	0,2565	0,025	16,193	14,6	fail	0,2565	0,025	16,193	14,6	fail	0,1805	0,0757	19,706	22,418	fail
V_{La0}	0,2417	0,0418	0,2072	5,2283	pass	0,2417	0,0418	0,2072	5,2283	pass	0,2417	0,4443	0,7664	13,015	fail
V_{La1}	0,152	0,0007	0,3723	7,3	pass	0,152	0,0007	0,3723	7,3	pass	0,1489	0,0752	1,5269	13,01	fail
V_{Lb0}	0,2220	0,0317	0,1664	5,2	pass	0,222	0,0317	0,1664	5,2	pass	0,2028	0,1163	0,4087	10,87	pass
V_{Lb1}	0,152	0,0007	0,2453	3,5411	pass	0,152	0,0007	0,2453	3,5411	pass	0,1608	0,0079	0,5841	5,2353	pass
$(V_{La}/V_{sa})_0$	1,3650	19,431	4,9005	5433,1	fail	0,5122	6,2985	1,8523	6,0046	pass	0,4049	5,2134	1,8523	7,8918	pass
$(V_{La}/V_{sa})_1$	0,0773	0,0303	0,772	26,01	fail	0,0773	0,0303	0,772	26,01	fail	0,1195	0,0259	0,9303	26,74	fail
$(V_{Lb}/V_{sb})_0$	1,0373	17,694	6,4297	4,3846	pass	0,9841	17,913	6,2926	4,0738	pass	0,8173	17,92	5,7197	5,3612	pass
$(V_{Lb}/V_{sb})_1$	0,0438	0,0205	0,5216	9,3733	pass	0,0438	0,0205	0,5216	9,3733	pass	0,0543	0,0181	0,6275	9,4	pass

Table 3

Parameters of the Rosin-Rammler distribution found by least-value methods of three different optimization functions

Sample	min [S]					min [χ_n^2]					min [$\lvert\delta\rvert$]				
	P_{80}	m	k, %	χ_n^2	p / f	P_{80}	m	k, %	χ_n^2	p / f	P_{80}	m	k, %	χ_n^2	p / f
V_{sa0}	0,1805	–2,386	1,7423	7,1642	pass	0,3056	–2,113	9,1709	4,7	pass	0,2109	–1,553	13,482	12,346	pass
V_{sa1}	0,0902	–2,151	5,7473	37,317	fail	0,0315	–1,586	3,21	14,3	fail	0,0688	–1,161	29,691	25,631	fail
V_{sa2}	0,0315	–1,586	11,352	2,9173	pass	0,0315	–1,586	11,352	2,9173	pass	0,0315	–1,586	11,352	2,9173	pass
V_{sb0}	0,2541	–2,365	3,1993	11,926	pass	0,3593	–1,987	12,585	6,9	pass	0,5663	–1,684	41,008	10,81	pass
V_{sb1}	0,0268	–2,032	0,4036	26,204	fail	0,0386	–1,577	3,2734	11,9	pass	0,0207	–1,321	3,2212	15,113	fail
V_{La0}	3,1312	–2,256	9,446	5,9963	pass	3,1485	–2,01	13,663	4,3	pass	2,0014	–1,535	14,892	10,414	pass
V_{La1}	0,3209	–1,759	1,7134	9,0664	pass	0,2343	–1,57	1,8828	6,7	pass	0,0545	–1,175	1,4054	12,782	fail
V_{Lb0}	4,7658	–2,172	17,249	6,0331	pass	9,3091	–2,054	64,144	5,0	pass	4,8744	–1,64	35,202	7,9189	pass
V_{Lb1}	0,6282	–1,774	3,2521	3,7653	pass	0,9564	–1,643	9,1006	2,9	pass	0,9436	–1,519	11,861	3,4959	pass
$(V_{La}/V_{sa})_0$	22,353	–3,877	140,96	19,576	fail	16,758	–2,465	143,2	4,861	pass	16,768	–2,225	153,39	5,925	pass
$(V_{La}/V_{sa})_1$	23,413	–4,757	274,1	3,6183	pass	21,604	–3,728	275,76	1,615	pass	21,751	–3,174	295,45	2,918	pass
$(V_{Lb}/V_{sb})_0$	14,942	–2,318	186,75	4,9948	pass	17,048	–2,613	195,52	4,663	pass	14,131	–2,215	183,03	5,269	pass
$(V_{Lb}/V_{sb})_1$	16,286	–2,381	289,31	1,8529	pass	17,945	–2,664	301,44	1,733	pass	16,182	–2,39	286,95	1,857	pass

Table 4

Parameters of the log-normal distribution found by least-value methods of three different optimization functions

Sample	min [S]					min [χ_n^2]					min [$\|\delta\|$]				
	α	μ	k, %	χ_n^2	p / f	α	μ	k, %	χ_n^2	p / f	α	μ	k, %	χ_n^2	p / f
V_{sa0}	8,6955	–103,7	$4{\cdot}10^{-31}$	7,309	pass	6,6476	–46,08	$1{\cdot}10^{-10}$	4,7	pass	6,2159	–17,82	0,1082	13,442	fail
V_{sa1}	18,404	–395,3	$9{\cdot}10^{-100}$	39,943	fail	49,085	–1365	$3{\cdot}10^{-168}$	14,23	fail	52,117	–394,6	$1{\cdot}10^{-12}$	24,06	fail
V_{sa2}	0,9723	–1,541	263,58	9,518	pass	10,205	–72,53	$8{\cdot}10^{-10}$	2,4384	pass	2,6315	–4,37	61,525	3,22	pass
V_{sb0}	24,509	–785,3	$1{\cdot}10^{-223}$	10,705	pass	5,5296	–27,49	$2{\cdot}10^{-5}$	6,9	pass	6,451	–19,36	0,062	12,971	fail
V_{sb1}	23,061	–559,1	$2{\cdot}10^{-127}$	29,516	fail	60,265	–1985	$6{\cdot}10^{-236}$	12,541	pass	$7{,}27{\cdot}10^{7}$	$2{,}71{\cdot}10^{7}$	$1{,}8{\cdot}10^{-6}$	29,51	fail
V_{La0}	20,409	–490,8	$3{\cdot}10^{-128}$	5,3465	pass	2,0235	–0,447	0,7664	5,0	pass	4,8108	–7,974	0,0998	10,885	pass
V_{La1}	19,56	–300,1	$1{\cdot}10^{-52}$	9,9285	pass	55,37	–1628	$1{\cdot}10^{-189}$	6,628	pass	15,135	–37,21	0,0348	12,773	fail
V_{Lb0}	3,936	–13,95	$1{,}2{\cdot}10^{-4}$	6,1062	pass	35,524	–1135	$2{\cdot}10^{-224}$	4,3916	pass	4,0878	–4,537	0,2195	9,6915	pass
V_{Lb1}	35,888	–1013	$4{\cdot}10^{-175}$	4,0159	pass	53,404	–1760	$6{\cdot}10^{-238}$	2,812	pass	4,1267	–4,297	0,731	4,6711	pass
$(V_{La}/V_{sa})_0$	0,5598	2,9365	6,028	98,108	fail	1,1351	2,5125	4,2804	5,6784	pass	2,2447	0,0739	1,1808	6,7514	pass
$(V_{La}/V_{sa})_1$	0,5845	2,8055	10,033	2,3175	pass	0,6167	2,8278	10,045	1,9421	pass	0,5339	2,7318	10,047	7,839	pass
$(V_{Lb}/V_{sb})_0$	0,8487	2,7798	7,699	3,0661	pass	0,7934	2,826	7,8837	4,0480	pass	0,98	2,8135	7,2359	5,0016	pass
$(V_{Lb}/V_{sb})_1$	0,7858	2,8143	2,023	11,356	pass	0,753	2,811	11,484	1,3663	pass	0,7623	2,6991	11,593	2,4707	pass

The following results emerge from the analysis of the data in Table 2 – 4.

1. Out of all 39 cases considered by the Pearson Chi-squared consistency criterion, the Weibull distribution passes in 25 cases, Rosin-Rammler in 32 cases, and the log-normal distribution in 30 cases.

2. Out of 18 cases considered for each of the three distributions for samples without screening out «anomalous» values by the Wright criterion, the following pass by the Pearson Chi-squared consistency criterion: the Weibull distribution in 14 cases, Rosin-Rammler in 17 cases, and log-normal in 15 cases.

3. For samples with one iteration of screening out «anomalous» values by the Wright criterion, out of 18 cases considered by the Pearson Chi-squared consistency criterion, the following pass: Weibull distribution in 8 cases, Rosin-Rammler and log-normal in 12 cases. For a sample with two iterations of screening out «anomalous» values according to the Wright criterion to the complete absence of areas with zero values, all distributions pass the Pearson Chi-squared consistency criterion in all cases. But the range of the random variable distribution in this case decreases by more than 6 times, which raises doubts about the feasibility of such screening.

4. The parameters found by the minimum values of the SSD (14) and Chi-squared (15) coincide in 12 cases out of 39. Perhaps this is due to the fact that both functions are built on absolute differences. The parameters found by the minimum values of (16) coincide with those found by other criteria only in 2 cases out of 39. Perhaps this is due to the fact that, unlike functions (14) and (15), function (16) uses relative, not absolute, estimates. Except for one case out of 39, the Chi-squared values for distributions whose parameters were found by the minimum value criterion (15) were less than or equal to the corresponding values for distributions whose parameter values were found by other criteria. This is logical and follows from the essence of the criterion for finding optimal values of distribution parameters by the minimum values of the function (15).

5. The values of the Chi-squared parameter found by the minimum value criterion of the Chi-squared function (15) for the Weibull distribution in samples without screening out «anomalous» values in 5 cases out of 6 were less than the corresponding values for samples with one iteration of screening out «anomalous» values. For the Rosin-Rammler and log-normal distributions, these values were distributed equally: 3 cases each for samples without screening out and with screening out.

6. Of all 13 samples, the Chi-squared values found by the criterion of the minimum value of the Chi-squared function (15) for the Weibull distribution were always greater than the corresponding values for the other distributions considered. The values of this parameter for the Rosin-Rammler and log-normal distributions coincided in 2 cases out of 13. In 7 cases out of 13 for the log-normal distribution, the values of this parameter were smaller than for the Rosin-Rammler distribution. Accordingly, in 4 cases out of 13, the values of this parameter for the Rosin-Rammler distribution were smaller than for the log-normal distribution.

7. For samples without screening out «anomalous» values, smaller values of the Chi-square parameter for the log-normal distribution were observed in 2 cases out of 6. In 2 cases out of 6, the value of this parameter coincided with the values found for the Rosin-Rammler distribution, and in 2 out of 6 cases, these values for the Rosin-Rammler distribution were smaller than the values for the log-normal distribution.

8. For samples with one iteration of screening out «anomalous» values, smaller values of the Chi-squared parameter for the log-normal distribution were observed in 4 cases out of 6, and for the Rosin-Rammler distribution – in 2 of 6. For the sample with two iterations of screening out «anomalous» values, the smallest values of the Chi-squared parameter were found for the log-normal distribution.

Summarizing the results of the above analysis, we note that of all the theoretical distributions considered, the Weibull distribution describes the discrete distributions obtained in practice the worst, and the log-normal one the best. Therefore, for it, the parameter values were also found by the method of statistical moments both from the input data and from the data of discrete distributions (Table 5).

Table 5

Parameters of the log-normal distribution, found by the methods of statistical moments from input data and discrete distributions

Sample	From input data					From discrete distribut.				
	α	μ	k, %	χ_n^2	p/f	α	μ	k, %	χ_n^2	p/f
V_{sa0}	1,433	–1,07	17,6	7,23	p	0,922	0,152	41,5	15,9	f
V_{sa1}	1,279	–1,17	86,6	31,4	f	1,053	–0,62	114	34,2	f
V_{sa2}	1,146	–1,78	222	5,66	p	0,951	–1,39	275	7,68	p
V_{sb0}	1,401	–0,83	17,6	9,51	p	0,917	0,317	38,5	16,9	f
V_{sb1}	1,289	–0,94	70,4	29,0	f	1,053	–0,41	93,0	33,1	f
V_{La0}	1,291	1,592	2,63	7,07	p	0,902	2,439	4,74	14,4	f
V_{La1}	1,146	1,549	9,61	18,2	f	0,956	1,924	11,5	21,6	f
V_{Lb0}	1,283	1,816	2,24	7,76	p	0,911	2,692	3,98	12,9	f
V_{Lb1}	1,151	1,765	7,09	11,1	p	0,959	2,187	8,65	13,3	f
$(V_{La}/V_{sa})_0$	0,848	2,722	5,27	8,92	p	0,829	2,759	5,36	9,07	p
$(V_{La}/V_{sa})_1$	0,628	2,727	10,3	3,84	p	0,607	2,743	10,2	3,41	p
$(V_{Lb}/V_{sb})_0$	0,687	2,756	8,23	6,68	p	0,670	2,768	8,27	7,09	p
$(V_{Lb}/V_{sb})_1$	0,606	2,750	11,9	3,97	p	0,596	2,755	11,9	4,32	p

Analysis of the data in Table 5 allows us to make the following generalizations.

1. In 12 out of 13 cases, the Chi-squared values for log-normal distributions, the parameters of which were found from the input data, were smaller than for similar distributions, the parameters of which were found from the data of discrete distributions. Only in one case the opposite situation was observed.

2. In all 6 cases considered, the log-normal distribution, the parameters of which were found from the input data without screening out «anomalous» values, passes the Pearson Chi-squared consistency criterion. The log-normal distribution, the parameters of which were found by the parameters of discrete distributions without screening out «anomalous» values according to the Pearson Chi-squared criterion, passes in 2 cases out of 6.

3. The log-normal distribution, the parameters of which were found by the input data with screening out «anomalous» values in one iteration passes by the Pearson Chi-squared consistency criterion in 3 out of 6 cases, and by the data of discrete distributions – in 2 cases out of 6.

From the above analysis it follows that for the considered samples the best results are shown by log-normal distributions, the parameters of which were found by the methods of statistical moments from the input data without screening out «anomalous» values.

Methodology for constructing distributions of the volumes of the components of plasma channels. One of the results of the above-described studies and analysis of the obtained data is the method of constructing distributions developed by us, which consists in the following.

1. To approximate the equivalent volumes of spark cores and colored halo of plasma channels, «flattened» ellipsoids of rotation are used.

2. «Anomalous» measurement results are not screened out.

3. To approximate the obtained discrete distributions, a continuous analytical log-normal distribution is used.

4. The parameters of the log-normal distribution are determined by the method of statistical moments according to (10) and (13) based on the input sample data without filtering out «anomalous» measurement results.

5. The hypothesis of the correspondence of theoretical distributions to the discrete distributions obtained in practice is checked using the Pearson Chi-squared consistency criterion.

6. To compare the quality of approximation of discrete distributions obtained in practice by continuous theoretical distributions, a universal dimensionless criterion is used – the average modulus of relative deviations of the values obtained during experiments of discrete and continuous theoretical distributions.

Comparative analysis of the distributions by the sizes of erosion particles and holes on the surface of granules and components of plasma channels. In [48] it is shown that the distribution of the diameters of spark erosion holes on the surface of aluminum granules is best described by the Rosin-Rammler distribution, and the particles obtained from them are best described by the normal distribution. The volume of a hole of average diameter in the hypothesis that it has the shape of a hemisphere is 15 % higher than the volume of a particle of average diameter in the hypothesis that it has the shape of a sphere. That is, the average parameters of erosion particles can be predicted by the average parameters of holes, but their diameter distributions are described by different laws and the maximum diameter of holes can be twice the maximum diameter of particles.

Therefore, the distributions of the volumes of colored halo plasma channels, their spark cores and their ratios are best described by the log-normal law, but can be described by the Rosin-Rammler law. The distribution of the diameters of erosion holes on the surface of the granules is described by the Rosin-Rammler law, and the distribution of the diameters of erosion particles is described by a normal distribution. That is, there is a probability that the correlation between the volumes of the constituent plasma channels and erosion holes on the surface of the granules is stronger than between the volumes of the constituent plasma channels and erosion particles. This suggests that the process of erosion particle formation is more complex than the condensation and solidification of the metal volume of one erosion particle from one erosion hole [53]. However, additional studies are needed to verify this.

Generalization and conclusions.

1. In the process of determining the volumes of spark cores and colored halo of plasma channels, they can be approximated with sufficient accuracy for statistical studies by ellipsoids of rotation. Judging by the quality of approximation by theoretical distributions of their size distributions obtained as a result of experiments in the hypotheses of «elongated» and «flattened» ellipsoids in the studied regimes, the probability of the appearance of «flattened» ellipsoids is higher than «elongated».

2. The distributions of the volumes of the components of the plasma channels and their ratios obtained as a result of measurements have a similar appearance and can be approximated by one theoretical distribution with different parameter values. Of all the theoretical distributions considered (Weibull, Rosin-Rammler and log-normal), the best approximation of the discrete distributions obtained as a result of measurements is provided by the log-normal, and the worst by Weibull.

3. Screening out «anomalous» measurement results according to the Wright criterion in the considered cases not only significantly narrows the range of distributions of random variables (more than 2 times with one iteration of screening and more than 6 times with two iterations), but also in the vast majority of cases leads to a deterioration in the quality of approximation of the discrete distributions obtained in practice by continuous theoretical distributions according to the Pearson Chi-squared consistency criterion. Therefore, in the considered conditions, it is impractical.

4. In most cases, the method of searching for optimal values of the parameters of the theoretical laws of distributions of random variables by the smallest deviation of theoretical values from the experimental results gives smaller Chi-squared values than the method of statistical moments. But the values of the distribution parameters found by the first method are not the only possible solution and do not always correspond to the physically determined ranges due to the redundancy of the systems of equations that are solved to find them.

5. Among all the considered optimization functions, the minimum values of which were used to find the optimal values of the parameters of the theoretical laws of the distribution of random variables by the method of the least deviations of theoretical values from the experimental results, the smallest values of the Chi squared are expected to be provided by the function based on the Pearson Chi squared consistency criterion.

6. The universality of the criterion for the quality of the approximation of distributions among all the considered functions is provided only by the average modulus of the relative deviations of the values of the discrete and continuous theoretical distributions obtained during the experiments, since it does not depend on either the number of intervals of the discrete distributions or the absolute values of the random variables.

7. The search for the values of the parameters of the theoretical laws of distributions of random variables by the statistical moments of the samples is more accurate than by the statistical moments of discrete distributions. The method of statistical moments ensures the uniqueness of the results and their correspondence to the physically determined ranges. In the case of consistency between the distributions obtained in practice and the theoretical one by the Pearson Chi squared criterion, the method of statistical moments ensures the finding of satisfactory values of the parameters of the theoretical distributions.

8. A method for constructing the volume distributions of the components of plasma channels has been developed, adapted specifically for such objects.

Acknowledgment. The work was carried out with the support of the Ministry of Education and Science of Ukraine (Project DB No. 0121U107443).

Conflict of interest. The authors of the article declare that there is no conflict of interest.

REFERENCES

1. Gilchuk A., Monastyrsky G. «Core–shell» nanoparticles produced from Ti-Ni-Hf and Ti-Ni-Zr alloys by spark erosion method. *Applied Nanoscience*, 2023, vol. 13, no. 11, pp. 7145-7154. doi: https://doi.org/10.1007/s13204-023-02864-9.

2. Jin C.H., Si P.Z., Xiao X.F., Feng H., Wu Q., Ge H.L., Zhong M. Structure and magnetic properties of Cr/Cr2O3/CrO2 microspheres prepared by spark erosion and oxidation under high pressure of oxygen. *Materials Letters*, 2013. vol. 92, pp. 213-215. doi: https://doi.org/10.1016/j.matlet.2012.10.126.

3. Berkowitz A.E., Hansen M.F., Parker F.T., Vecchio K.S., Spada F.E., Lavernia E.J., Rodriguez R. Amorphous soft magnetic particles produced by spark erosion. *Journal of Magnetism and Magnetic Materials*, 2003, vol. 254-255, pp. 1-6. doi: https://doi.org/10.1016/S0304-8853(02)00932-0.

4. Aur S., Egami T., Berkowitz A.E., Walter J.L. Atomic Structure of Amorphous Particles Produced by Spark Erosion. *Physical Review B*, 1982, vol. 26, no. 12, pp. 6355-6361. doi: https://doi.org/10.1103/PhysRevB.26.6355.

5. Hong J.I., Parker F.T., Solomon V.C., Madras P., Smith D.J., Berkowitz A.E. Fabrication of spherical particles with mixed amorphous/crystalline nanostructured cores and insulating oxide shells. *Journal of Materials Research*, 2008, vol. 23, no. 06, pp. 1758-1763. doi: https://doi.org/10.1557/JMR.2008.0199.

6. Perekos A.E., Chernenko V.A., Bunyaev S.A., Zalutskiy V.P., Ruzhitskaya T.V., Boitsov O.F., Kakazei G.N. Structure and magnetic properties of highly dispersed Ni-Mn-Ga powders prepared by spark-erosion. *Journal of Applied Physics*, 2012, vol. 112, no. 9. art. no. 093909. doi: https://doi.org/10.1063/1.4764017.

7. Harrington T., McElfresh C., Vecchio K.S. Spark erosion as a high-throughput method for producing bimodal nanostructured 316L stainless steel powder, *Powder Technology,* 2018, vol. 328, pp. 156–166. doi: https://doi.org/10.1016/j.powtec.2018.01.012.

8. Wang W., Zhu F., Weng J., Xiao J., Lai W. Nanoparticle morphology in a granular Cu–Co alloy with giant magnetoresistance, *Applied Physics Letters*, 1998, vol. 72, no 9, pp. 1118–1120. doi: https://doi.org/10.1063/1.120942.

9. Berkowitz A.E., Walter J.L. Spark Erosion: A Method for Producing Rapidly Quenched Fine Powders, *Journal of Materials Research*. 1987, no 2. pp. 277–288. doi: https://doi.org/10.1557/JMR.1987.0277.

10. Shen B., Inoue A. Fabrication of large-size Fe-based glassy cores with good soft magnetic properties by spark plasma sintering*, Journal of Materials Research,* 2003, vol. 18, no 9, pp. 2115–2121. doi: https://doi.org/10.1557/jmr.2003.0297.

11. Youssef F.S., El-Banna H.A., Elzorba H.Y., Gabal A.M. Application of Some Nanoparticles in the Field of Veterinary Medicine, *International Journal of Veterinary Science and Medicine*, 2019, vol. 7, no 1. pp. 78-93. doi: https://doi.org/10.1080/23144599.2019.1691379.

12. Batsmanova L., Taran N., Konotop Ye., Kalenska S., Novytska N. Use of a Colloidal Solutions of Metal and Metal Oxide-Containing Nanoparticles as Fertilizer for Increasing Soybean Productivity, *Journal of Central European Agriculture*, 2020, no 2 (21), pp. 311–319. doi: https://doi.org/10.5513/JCEA01/21.2.2414.

13. Petrov O., Petrichenko S., Yushchishina A., Mitryasova O., Pohrebennyk V. Electrospark Method in Galvanic Wastewater Treatment for Heavy Metal Removal. *Applied Sciences*, 2020, vol. 10, no. 15, art. no. 5148. doi: https://doi.org/10.3390/app10155148.

14. Goncharuk V.V., Shcherba A.A., Zakharchenko S.N., Savluk O.S., Potapchenko N.G., Kosinova V.N. Disinfectant action of the volume electrospark discharges in water. *Khimiia i tehnologiia vody*, 1999, vol. 21, no. 3, pp. 328-336. (Rus).

15. Shydlovska N.A., Zakharchenko S.M., Zakharchenko M.F., Mazurenko I.L., Kulida M.A. Physical and Technical-economic Aspects of Modern Methods of Water Treatment for Thermal and Nuclear Power Engineering. *Technical Electrodynamics*, 2022, no. 4, pp. 69-77. (Ukr). doi: https://doi.org/10.15407/techned2022.04.069.

16. Zakharchenko S.N., Kondratenko I.P., Perekos A.E., Zalutsky V.P., Kozyrsky V.V., Lopatko K.G. Influence of discharge pulses duration in a layer of iron granules on the size and structurally-phase conditions of its electroerosion particles. *Eastern-European Journal of Enterprise Technologies*, 2012. vol. 6, no. 5 (60), pp. 66-72. (Rus).
17. Shydlovska N.A., Zakharchenko S.M., Cherkaskyi O.P. Physical Prerequisites of Construction of Mathematical Models of Electric Resistance of Plasma-erosive Loads. *Technical Electrodynamics*, 2017, no 2, pp. 5-12. (Ukr) doi: https://doi.org/10.15407/techned2017.02.005.
18. Shydlovska N.A., Zakharchenko S.M., Cherkassky O.P. The Analysis of Electromagnetic Processes in Output Circuit of the Generator of Discharge Pulses with Non-linear Model of Plasma-erosive Load at Change Their Parameters in Wide Ranges. *Technical Electrodynamics*, 2016, no. 1. pp. 87-95. (Rus). doi: https://doi.org/10.15407/techned2016.01.087.
19. Shydlovska N.A., Zakharchenko S.M., Cherkaskyi O.P. Parametric model of resistance of plasma-erosive load, adequate in the wide range of change of applied voltage. *Technical Electrodynamics*, 2017, no 3, pp. 3-12. (Ukr) doi: https://doi.org/10.15407/techned2017.03.003.
20. Shydlovskaya N.A., Zakharchenko S.N., Cherkasskyi A.P. Nonlinear-parametrical model of electrical resistance of current-carrying granulated mediums for a wide range of applied voltage. *Technical Electrodynamics*, 2014, no 6, pp. 3-17. (Rus).
21. Zakharchenko S.M., Perekos A.O., Shydlovska N.A., Ustinov A.I., Boytsov O.F., Voynash V.Z. Electrospark Dispersion of Metal Materials. I. Influence of Velocity of Flow of Operating Fluid on Dispersity of Powders. *Metallofizika i Noveishie Tekhnologii*, 2018, vol. 40, no. 3, pp. 339-357 (Rus). doi: https://doi.org/10.15407/mfint.40.03.0339.
22. Carrey J., Radousky H.B., Berkowitz A.E. Spark-eroded particles: influence of processing parameters. *Journal of Applied Physics*, 2004, vol. 95, no. 3, pp. 823-829. doi: https://doi.org/10.1063/1.1635973.
23. Suprunovska N.I., Shcherba M.A., Roziskulov S.S., Synytsyn V.K. Improving the dynamic characteristics of electric discharge installations, which are significantly distant from the spark-erosion load. *Technical Electrodynamics*, 2022, no 3, pp. 16-21. doi: https://doi.org/10.15407/techned2022.03.016.
24. Kornev I., Saprykin F., Lobanova G., Ushakov V., Preis S. Spark erosion in a metal spheres bed: Experimental study of the discharge stability and energy efficiency. *Journal of Electrostatics*, 2018, vol. 96, pp. 111-118. doi: https://doi.org/10.1016/j.elstat.2018.10.008.
25. Gnedenko B.V. *Theory of Probability*. London, Routledge, 1998. 520 p. doi: https://doi.org/10.1201/9780203718964.
26. Shydlovska N.A., Zakharchenko S.M., Zakharchenko M.F., Kulida M.A., Zakusilo S.A. Spectral and optic-metric methods of monitoring parameters of plasma channels caused by discharge currents between metals granules in working liquids. *Electrical Engineering & Electromechanics*, 2024, no. 6, pp. 72-83. doi: https://doi.org/10.20998/2074-272X.2024.6.10.
27. Kim C.J. Electromagnetic Radiation Behavior of Low-Voltage Arcing Fault. *IEEE Transactions on Power Delivery*, 2009, vol. 24, no. 1, pp. 416-423. doi: https://doi.org/10.1109/TPWRD.2008.2002873.
28. Kozioł M., Nagi Ł., Kunicki M., Urbaniec I. Radiation in the Optical and UHF Range Emitted by Partial Discharges. *Energies*, 2019, vol. 12, no. 22, art. no. 4334. doi: https://doi.org/10.3390/en12224334.
29. Kozioł M. Energy Distribution of Optical Radiation Emitted by Electrical Discharges in Insulating Liquids. *Energies*, 2020, vol. 13, no. 9, art. no. 2172. doi: https://doi.org/10.3390/en13092172.
30. Kohut A., Ludvigsson L., Meuller B.O., Deppert K., Messing M.E., Galbács G., Geretovszky Z. From plasma to nanoparticles: optical and particle emission of a spark discharge generator. *Nanotechnology*, 2017, vol. 28, no. 47, art. no. 475603. doi: https://doi.org/10.1088/1361-6528/aa8f84.
31. Korytchenko K.V., Essmann S., Markus D., Maas U., Poklonskii E.V. Numerical and Experimental Investigation of the Channel Expansion of a Low-Energy Spark in the Air. *Combustion Science and Technology*, 2019, vol. 191, no. 12, pp. 2136-2161. doi: https://doi.org/10.1080/00102202.2018.1548441.
32. Lo A., Cessou A., Lacour C., Lecordier B., Boubert P., Xu D., Laux C.O., Vervisch P. Streamer-to-spark transition initiated by a nanosecond overvoltage pulsed discharge in air. *Plasma Sources Science and Technology*, 2017, vol. 26, no. 4. art. no. 045012. doi: https://doi.org/10.1088/1361-6595/aa5c78.
33. Mylnikov D., Efimov A., Ivanov V. Measuring and optimization of energy transfer to the interelectrode gaps during the synthesis of nanoparticles in a spark discharge. *Aerosol Science and Technology*, 2019, vol. 53, no. 12, pp. 1393-1403. doi: https://doi.org/10.1080/02786826.2019.1665165.
34. Raizer Yu.P. *Gas Discharge Physics*. Berlin, Springer, 1991. 449 p.
35. Baranov M.I. A generalized physical principle of development of plasma channel of a high-voltage pulse spark discharge in a dielectric. *Electrical Engineering & Electromechanics*, 2024, no. 1, pp. 34-42. doi: https://doi.org/10.20998/2074-272X.2024.1.05.
36. Korytchenko K.V., Shypul O.V., Samoilenko D., Varshamova I.S., Lisniak A.A., Harbuz S.V., Ostapov K.M. Numerical simulation of gap length influence on energy deposition in spark discharge. *Electrical Engineering & Electromechanics*, 2021, no. 1, pp. 35-43. doi: https://doi.org/10.20998/2074-272X.2021.1.06.
37. *ToupTek. Download*. Available at: https://www.touptekphotonics.com/download/ (Accessed: 28 June 2024).
38. Mishra P., Pandey C., Singh U., Gupta A., Sahu C., Keshri A. Descriptive statistics and normality tests for statistical data. *Annals of Cardiac Anaesthesia*, 2019, vol. 22, no. 1, pp. 67-72. doi: https://doi.org/10.4103/aca.ACA_157_18.
39. Arya R., Antonisamy B., Kumar S. Sample Size Estimation in Prevalence Studies. *The Indian Journal of Pediatrics*, 2012, vol. 79, no. 11, pp. 1482-1488. doi: https://doi.org/10.1007/s12098-012-0763-3.
40. Akagawa S., Odagaki T. Geometrical percolation of hard-core ellipsoids of revolution in the continuum. *Physical Review E*, 2007, vol. 76, no. 5, art. no. 051402. doi: https://doi.org/10.1103/PhysRevE.76.051402.
41. Menzies N.A. An Efficient Estimator for the Expected Value of Sample Information. *Medical Decision Making*, 2016, vol. 36, no. 3, pp. 308-320. doi: https://doi.org/10.1177/0272989X15583495.
42. Wu Z., Yang X., Tu J., Chen X. Optimal consistency and consensus models for interval additive preference relations: A discrete distribution perspective. *Journal of the Operational Research Society*, 2020, vol. 71, no. 9, pp. 1479-1497. doi: https://doi.org/10.1080/01605682.2019.1621219.
43. Burshtynska H.V., Yidunov A.V. The study of various statistical criteria in the processing of false points in the process of determining the elements of mutual orientation. *Geodesy, Cartography and Aerial Photography*, 1984, no. 39, pp. 114-118. (Rus).
44. Adikaram K.K.L.B., Hussein M.A., Effenberger M., Becker T. Data Transformation Technique to Improve the Outlier Detection Power of Grubbs' Test for Data Expected to Follow Linear Relation. *Journal of Applied Mathematics*, 2015, vol. 2015, art. no. 708948. doi: https://doi.org/10.1155/2015/708948.
45. Zhao Y., Lehman B., Ball R., Mosesian J., de Palma J.-F. Outlier detection rules for fault detection in solar photovoltaic arrays. *2013 Twenty-Eighth Annual IEEE Applied Power*

Electronics Conference and Exposition (APEC), 2013, pp. 2913-2920. doi: https://doi.org/10.1109/APEC.2013.6520712.
46. Barbato G., Barini E.M., Genta G., Levi R. Features and performance of some outlier detection methods. *Journal of Applied Statistics*, 2011, vol. 38, no. 10, pp. 2133-2149. doi: https://doi.org/10.1080/02664763.2010.545119.
47. Ventzel E.S. *Theory of Probability*. Moscow, Nauka Publ., 1969. 576 p. (Rus).
48. Shidlovska N.A., Zakharchenko S.M., Perekos A.O. Peculiarities of the diameter distributions obtained at submilisecond duration of discharge pulses spark-erosive aluminum particles and caverns on the surface of its granules. *Technical Electrodynamics*, 2021, no. 1, pp. 10-22. (Ukr). doi: https://doi.org/10.15407/techned2021.01.010.
49. Mitzenmacher M. A brief history of generative models for power law and lognormal distributions. *Internet Mathematics*, 2004, vol. 1, no. 2, pp. 226-251. doi: https://doi.org/10.1080/15427951.2004.10129088.
50. Cuff V., Lewis A., Miller S.J. The Weibull distribution and Benford's law. *Involve, a Journal of Mathematics*, 2015, vol. 8, no. 5, pp. 859-874. doi: https://doi.org/10.2140/involve.2015.8.859.
51. Kumar R., Gopireddy S.R., Jana A.K., Patel C.M. Study of the discharge behavior of Rosin-Rammler particle-size distributions from hopper by discrete element method: A systematic analysis of mass flow rate, segregation and velocity profiles. *Powder Technology*, 2020, vol. 360, pp. 818-834. doi: https://doi.org/10.1016/j.powtec.2019.09.044.
52. Franke T.M., Ho T., Christie C.A. The Chi-Square Test: Often Used and More Often Misinterpreted. *American Journal of Evaluation*, 2012, vol. 33, no. 3, pp. 448-458. doi: https://doi.org/10.1177/1098214011426594.
53. Kucheriava I.M. Multiphysics processes at spark erosion treatment of conducting granules. *Technical Electrodynamics*, 2017, no. 5, pp. 32-38. (Rus). doi: https://doi.org/10.15407/techned2017.05.032.

Received 03.07.2024
Accepted 20.08.2024
Published 02.01.2025

N.A. Shydlovska[1], *Corresponding Member of NAS of Ukraine, Doctor of Technical Science, Chief Research Scientist,*
S.M. Zakharchenko[1], *Doctor of Technical Science, Leading Research Scientist,*
M.F. Zakharchenko[2], *Candidate of Chemical Sciences,*
M.A. Kulida[3], *Candidate of Veterinary Sciences,*
S.A. Zakusilo[1], *Postgraduate Student,*
R.A. Yakovenko[1], *Postgraduate Student,*
[1] Institute of Electrodynamics
of the National Academy of Sciences of Ukraine,
56, Prospect Beresteiskyi, Kyiv, 03057, Ukraine,
e-mail: snzakhar@ukr.net (Corresponding Author)
[2] V.I. Vernadsky Institute of General and Inorganic Chemistry
of the National Academy of Sciences of Ukraine,
32/34, Prospect Palladina, Kyiv, 03142, Ukraine.
[3] National University of Life and Environmental Sciences of Ukraine,
16, Vystavkova Str., Kyiv, 03041, Ukraine.

How to cite this article:
Shydlovska N.A., Zakharchenko S.M., Zakharchenko M.F., Kulida M.A., Zakusilo S.A., Yakovenko R.A. Distribution of volumes of plasma channels components between metal granules in working liquids. *Electrical Engineering & Electromechanics*, 2025, no. 1, pp. 73-85. doi: https://doi.org/10.20998/2074-272X.2025.1.10